A New Method of Multiplanar Emission Tomography Using a Seven Pinhole Collimator and an Anger Scintillation Camera

Robert A. Vogel, Dennis Kirch, Michael LeFree, and Peter Steele

Denver Veterans Administration Hospital, Denver, Colorado

A new method of multiplanar emission tomography is described; it uses a wide-field Anger scintillation camera (37.5 cm crystal diameter) and a seven-pinhole collimator. The pinholes (5.5 mm) acquire data simultaneously from the emissing source and project the data onto seven independent regions of the camera crystal. Multiple planes are reconstructed from the initial seven-view data acquisition through the use of a computerized addition-multiplication algorithm and variation of the superposition relationships among the projected views. These planes are then altered iteratively by a least-error criterion following ray-sum comparison with the original views. Planar resolution (full-width-half-maximum) is 1.0 cm and depth resolution is 1.5 cm. In 42 patients with angiographically demonstrated coronary-artery disease, studies of myocardial Tl-201 perfusion, under exercise, have shown improved detection sensitivity in comparison with scintigraphy using parallel-hole collimation.

J Nucl Med 19: 648–654, 1978

In contrast to the development of computerized transmission axial tomography, which has resulted in widespread clinical application, emission tomography has shown only modest clinical usefulness. This is despite the introduction of radionuclide tomographic scanning by Kuhl and Edwards 14 years ago (1) and of tomography by scintillation-camera techniques by Muehllehner 7 years ago (2). This report describes a new emission tomographic technique using a standard Anger scintillation camera (crystal 37.5 cm in diameter) and a seven-pinhole collimator that views simultaneously seven independent projections of a volume of interest. An iterative computer algorithm is used to reconstruct multiple planes through the volume of interest. Clinical tomographic images obtained by this method are shown to be superior to corresponding nontomographic scintigraphic images.

METHODS

Description of collimator. A lead collimator was constructed with seven pinholes, 5.5 mm in diameter, placed in a plane parallel to and 12.7 cm from the camera crystal (Fig. 1). The centers of the six peripheral pinholes are 6.35 cm from the axial pinhole and from each other in a hexagonal pattern. Figure 2 shows the lead shielding located between the pinhole plane and the crystal; it prevents overlap of projected pinhole images on the detector. The central collimator pinhole has a conical field of view of 53° apical angle. The outer holes have conical fields of view of 45°. The central conical field of view is perpendicular to the crystal face, whereas the longitudinal axes of the peripheral conical fields converge inward at 26.5°. Thus, a conically tipped cylindrical volume, 12.7 cm in diameter, is formed within which emissive data project through all seven pinholes simultaneously onto seven independent crystal sectors, each viewing the volume from a different spatial angle. The mean angle between views from opposite peripheral pinholes is 53° and the
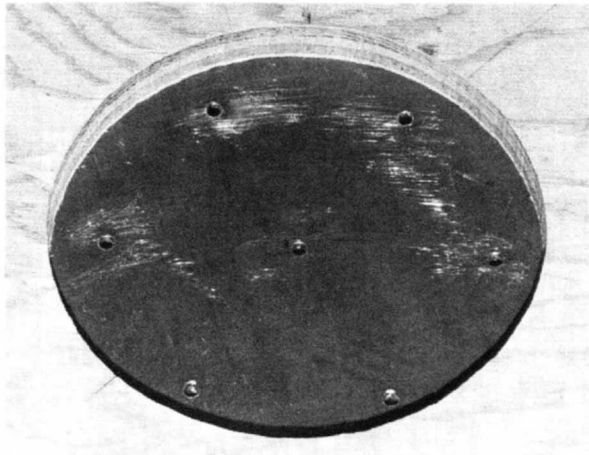
FIG. 1. Close-up view of tomographic collimator showing detail of seven-pinhole array. Pinholes are 5.5 mm in diameter.

angle between the central view and each peripheral view is 26.5°.

Emissive data within any plane parallel to the collimator face project to the crystal as seven geometrically identical inverted images whose size relative to the emissing source is dependent upon the source's distance from the collimator. Additionally, image data more distant along a line perpendicular to the collimator face project more centrally within the peripheral crystal sectors, whereas more proximal image data project toward the outer edges of these crystal sectors.

Image reconstruction algorithm. Each scintigraphic study consisted of an initial single-projection acquisition of 750,000 Tl-201 counts using the compound collimator. A wide-field Anger camera was used, with an asymmetric, 30% energy window set with the lower energy limit roughly above the backscatter
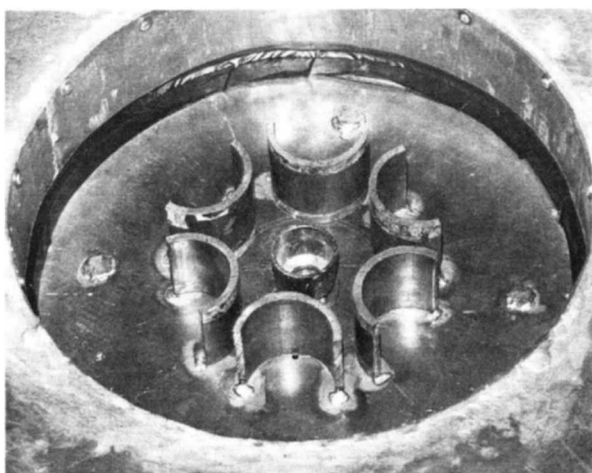
FIG. 2. Inside of tomographic collimator head showing lead shielding used to prevent images projected through each pinhole from overlapping.

peak to decrease the significant amounts of scatter otherwise present. Following the data acquisition, a second scintigram was obtained from point source (30,000-counts, from technetium-99m) centered 8.9 cm from the collimator face. This provided (for the 8.9-cm plane) a corresponding reference point of projection within each of the seven views. Lastly, a third scintigram (2,500,000 counts with similar energy peaking) was obtained from a 5-mCi Tc-99m planar flood source. This was used to correct for sensitivity distortion caused by pinhole imaging and use of the asymmetric energy window. All data were recorded on a tape recorder.

Using a digital computer*, the initial scintigraphic data within each of the seven crystal sectors were separately digitized centered about the location determined by the reference-point projection, then flood-corrected for sensitivity distortion, and then stored in 64- $\times$ 64-pixel disk memory. Opposite peripheral images were summed in a pixel-by-pixel fashion and a composite image was formed by taking the mathematical product, pixel by pixel, of these three peripheral summed images and the central image. Ten more-distant planes at 1.1 cm separation were then reconstructed by shifting the relative correspondence of the peripheral images increasingly outward. The entire 11-cm-deep by about 12-cm-diameter cylindrical volume of interest was reconstructed in this manner.

Using these initial reconstructed planes, ray-sum images corresponding to the original seven views were formed by appropriate shifting and addition of the planes to simulate the original viewing process. The differences between the ray-sum and the original views were used to modify the original views. A subsequent set of planes was reconstructed using the modified views, and the iterative process was repeated from 5 to 10 times recording the summed squares of the errors between the ray-sum images and the original views. The procedures was terminated after a 90% reduction in squared errors.

Resolution measurements. Using the above technique, full-width-half-maximum resolution measurements were made using a line source (1-mm capillary tube) of thallium-201 located 8.9, 12.7, and 16.5 cm from the collimator, with 5 cm of tissue-equivalent scattering material interposed. Additionally, standard 6-, 9-, 12-, and 25-mm parallel alternating bar-and-space phantoms were placed over a cobalt-57 flood source and imaged at 12.7 cm from the collimator.

Phantom measurements. A cardiac phantom was constructed consisting of three 270° arc segmental rings, 7, 8.5, and 10 cm in diameter and filled with Tc-99m solution. Ring width was 1.0 cm and depth

was 1.5 cm. Using a general-purpose parallel-hole collimator (2.5 cm thick), a scintigram of the three fluid filled rings was made (Fig. 3C). Two tomographic studies of these Tc-99m-filled rings were made with the rings stacked on top of each other. Figure 3C indicates the order of stacking (1 top, 2 middle, 3 bottom), with the open segment of each ring oriented as shown in Fig. 3C. Studies were done with no separation between the rings and with 1.5 cm separation, with a 1-cm layer of water interposed between the rings. Corresponding scintigrams with parallel-hole collimation (500,000 counts) were obtained from both phantoms.

Clinical studies. Forty-two informed and consenting patients underwent graded treadmill exercise testing (Bruce protocol) with four-lead electrocardiographic monitoring. Sixteen of them had angiographically normal coronary arteries and 26 had greater than 70% stenosis of at least one major coronary artery. Exercise was terminated at 85% of age-predicted maximum heart rate, or upon development of 1 mm of new ST-segment depression. Thirty seconds before the termination of exercise, 1.5 mCi of Tl-201 were injected intravenously. Ten minutes later, a single 40° left anterior oblique tomographic scintigram was obtained, followed immedi-
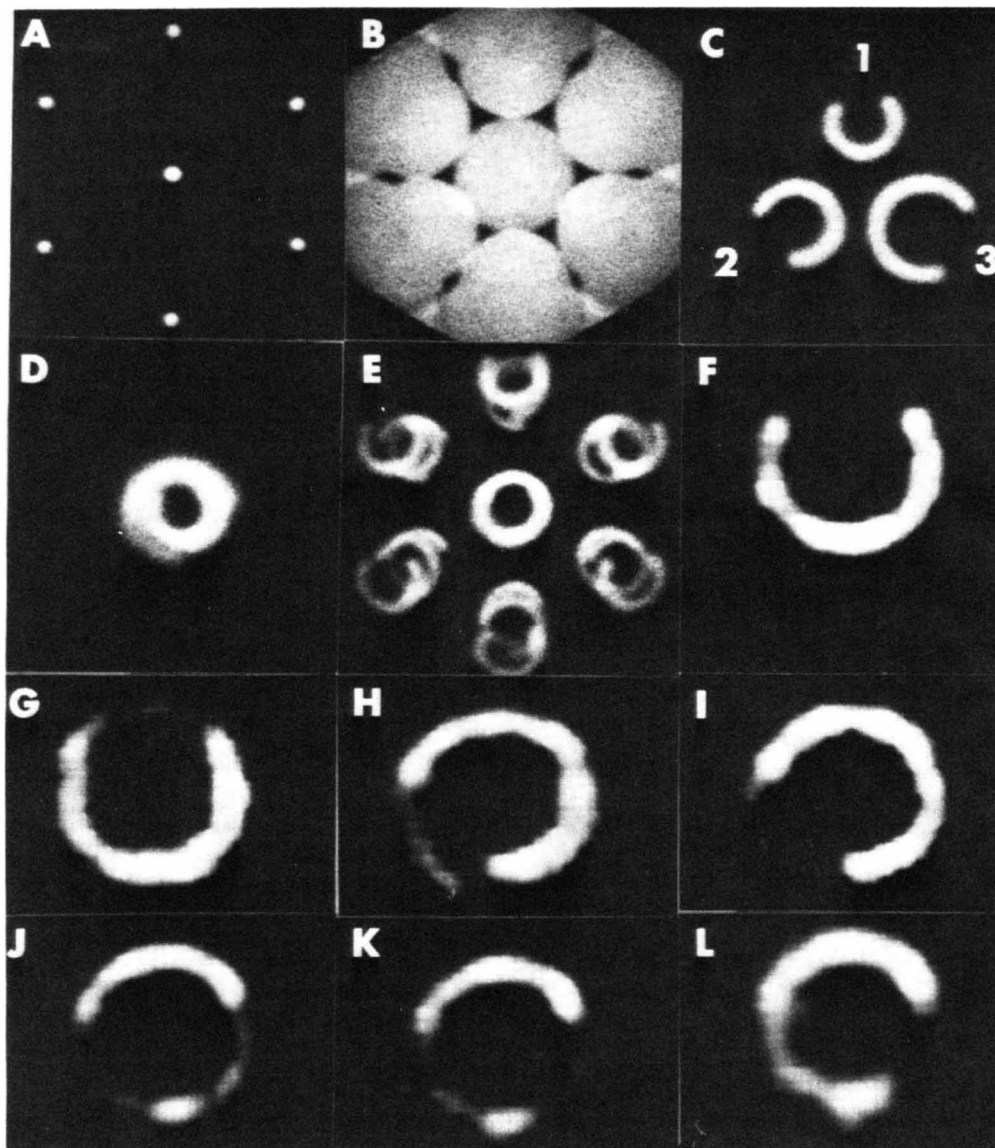
FIG. 3. (A) Pinhole-collimator image of a small Tc-99m source. (B) Pinhole-collimator image of Tc-99m flood source, showing nonuniformity of planar sensitivity. (C) Parallel-hole-collimator image of three rings composing cardiac phantom. (D) Parallel-hole image of ring phantom, composed of ring 1 top, ring 2 middle, and ring 3 bottom, stacked with 1.5-cm separation and 1 cm of water between rings. (E) Pinhole-collimator image of ring phantom. (F–L) Tomographic images of ring phantom with 1.1-cm separation proceeding distally from collimator.
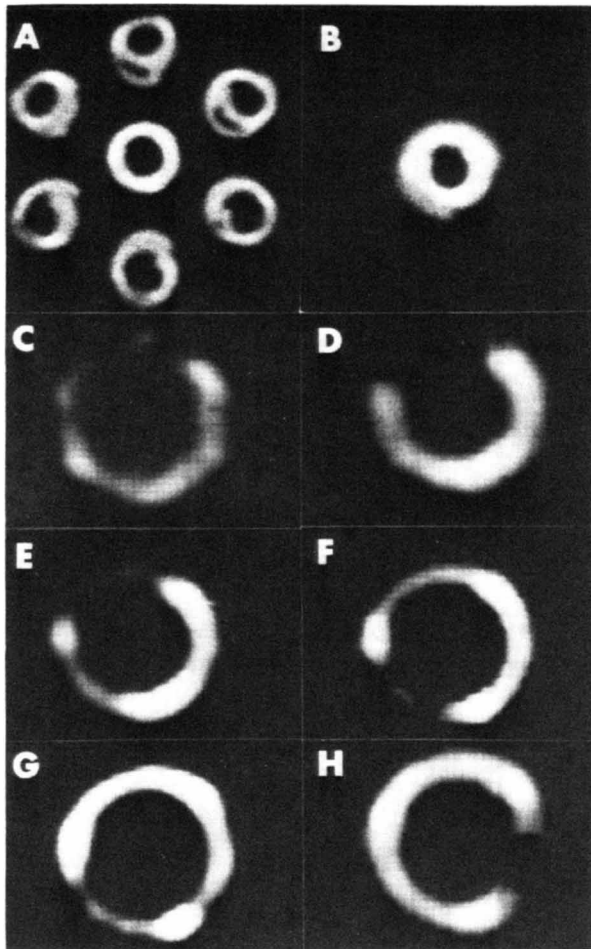
FIG. 4. (A) Composite pinhole-collimator image of ring phantom with same orientation as in Fig. 3, but with no separation between rings. (B) Parallel-hole image of same ring phantom. (C–H) Tomographic images of ring phantom with 1.1-separation proceeding distally from collimator.

ately by antero-posterior and 40° left anterior oblique scintigrams with parallel-hole collimation (general purpose). Eleven tomographic planes spaced approximately 1.1 cm apart were reconstructed through the cardiac region and were photographed from the computer display. An abnormal exercise tomographic study was defined as one having at least one plane demonstrating good cardiac-cavity visualization with at least a 55% difference between minimum and maximum regional count densities following uniform background subtraction (apical region excluded). The background value was obtained from a region directly below the apex in each plane, separated from the heart by a distance equal to the thickness of the cardiac wall. An abnormal exercise scintigram with parallel-hole collimation was defined as one demonstrating at least 30% difference between minimum and maximum regional count densities without background subtraction, the apical

region also excluded. Minimum-to-maximum count-density criteria for abnormality were arrived at as being just above the maximum values obtained from the first 15 normal individuals: 29% for standard imaging and 54% for tomographic imaging.

RESULTS

Resolution measurements. Full-width-half-maximum resolution using the Tl-201 line source was found to be 1.0 cm throughout a plane parallel to and 12.7 cm from the collimator; depth resolution (perpendicular to the collimator) was found to be 1.5 cm at that distance. Resolution was improved in closer planes and decreased for more distant ones, planar FWHM resolution being 0.8 cm at 8.9 cm distance and 1.4 cm at 16.5 cm. Six-millimeter bars spaced 6 mm apart could be easily distinguished scintigraphically at the same distance.

Phantom studies. Figures 3A and B show the seven pinhole-collimation images of the reference-point and flood sources, respectively. Figures 3D and E show the parallel-hole image and the seven pinhole-collimation images of the cardiac phantom, respectively, with the 270° arc rings spaced 1.5 cm apart. Figures 3F through 3L show the reconstructed planes proceeding distally from the camera at 1.1-cm intervals. Similarly, Fig. 4 shows images of the cardiac phantom with no spacing between the rings, with Figs. 4C through H showing the planes proceeding distally from the collimator at 1.1-cm separation.

Clinical studies. One of the 16 normal patients had an abnormal parallel-hole study and none had an abnormal tomographic study. Of these, the largest variation between minimum and maximum regional count densities, excluding the apical region, was 32% nontomographically and 54% tomographically. Figure 5 shows the seven pinhole, parallel-hole collimation, and reconstructed planar tomograms of a typical normal individual. Of the 26 patients with coronary-artery disease, 19 had abnormal parallel-hole scintigrams and 24 had abnormal tomographic studies. Figure 6 was obtained from an individual with 90% right and circumflex coronary-artery stenoses. Despite the normal appearance of the nontomographic image (6B), the tomographic planes demonstrate a perfusion defect in the posterior myocardial wall and a larger-than-usual apical defect.

DISCUSSION

Although the described tomographic technique with seven-pinhole collimation uses a process conceptually similar to other tomographic methods, the use of a single wide-field Anger scintillation camera to obtain simultaneously multiple independent viewing projections has not been previously described.

Coded-aperture technique does not provide independent views, and rotating collimation does not provide simultaneous views. The development of this technique was motivated by the need for improved cardiac imaging, since scintigraphy with parallel-hole collimation is compromised when viewing a relatively small spherical organ with significant background (lung) and rapid organ motion. The field of view approximately 12 cm in diameter has been found sufficient for all normal and abnormal hearts imaged to date. The 750,000-count original pinhole images were obtained in about 600 sec, compared with about 500 sec for equivalent single-projection studies with parallel-hole collimation. Moreover, the technique uses generally available resources—namely the Tl-201 radionuclide, a standard Anger scintillation camera, and a digital computer. Addition of the seven-pinhole collimator enables a laboratory with such facilities to perform tomographic imaging,

in a dynamic, gated, or constant-acquisition fashion.

The choice of pinhole collimation was based upon its resolution characteristics at the 10- to 20-cm distance from the collimator face as is required for multiple-projection viewing of intrathoracic structures. An initial trial using a multi-sectorial, parallel-hole collimator of foil construction resulted in considerably reduced image resolution. Pinhole collimation, however, introduces three variables not present using parallel-hole collimation: namely nonuniformity of planar and distance sensitivity and distance-related distortion of image size. Nonuniform planar sensitivity is eliminated by flood-source correction. The effect of decreasing pinhole planar sensitivity with increasing distance from the collimator is partially balanced by the reduction in projected image size associated with increasing distance from the collimator, tissue absorption not considered. Recently, a distance-variable weighting factor was
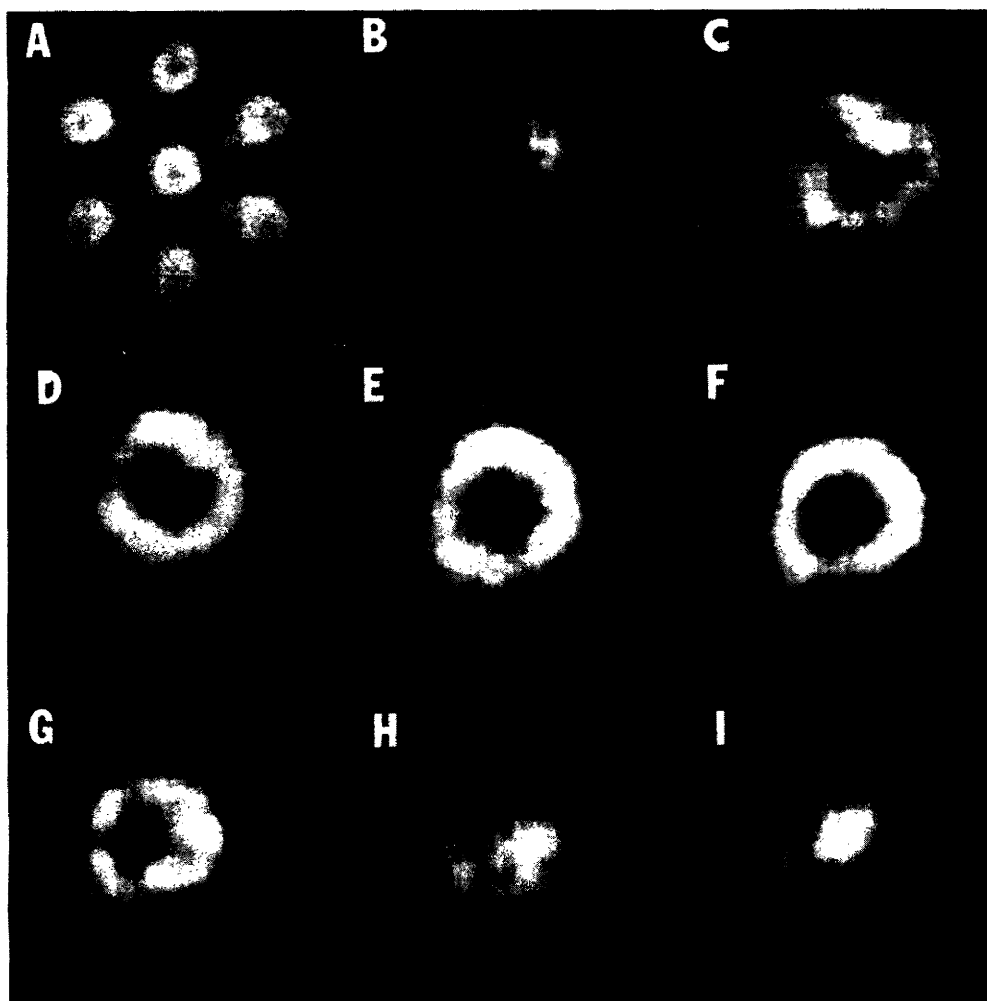
FIG. 5. (A) Pinhole-collimator image of a Tl-201 myocardial perfusion study in an exercised individual with normal coronary arteries, taken in the 40° left anterior oblique projection. (B–I) Tomographic images of same subject with 1.1-cm separation proceeding distally from collimator.
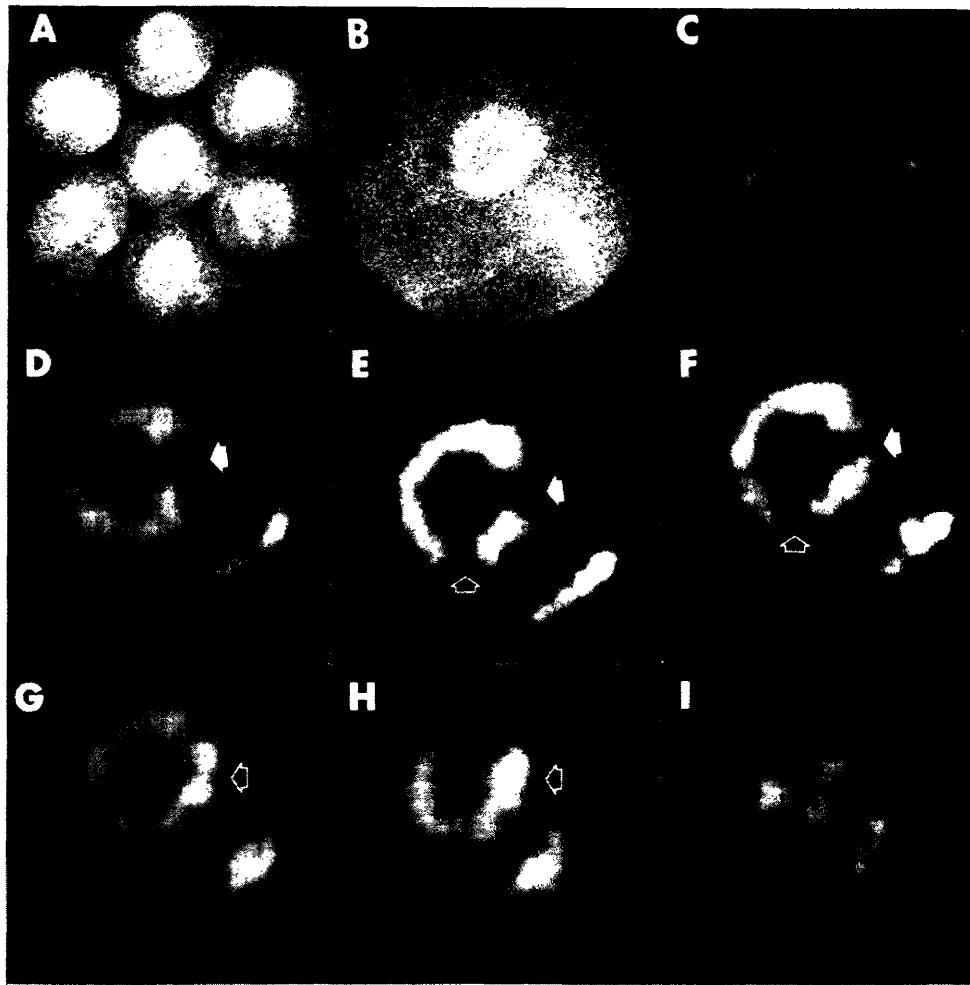
FIG. 6. (A) Pinhole-collimator image of a Tl-201 myocardial perfusion study in an exercised individual with 90% right and circumflex coronary-artery stenoses, taken in 40° left anterior oblique projection. (B) Parallel-hole image of same patient taken in same projection. (C-I) Tomographic images of same patient with 1.1-cm separation proceeding distally from collimator. Despite normal appearance of Fig. 6B, Fig. 6D-F show significantly decreased posterior myocardial-wall perfusion (solid arrows). A larger than usual apical myocardial-wall perfusion defect is seen in Figs. 6E and F (open arrows). Areas of above-normal posterior myocardial-wall perfusion are seen in Figs. 6G and H (open arrows); these would tend to conceal the defect in the nontomographic image.

added to the ray-summing portion of the reconstruction algorithm to correct for photon absorption by tissue, although the data presented did not employ this technique. Lastly, due to the tomographic visualization of planes parallel to the collimator face, distance-related image-size variation does not enter into single-section interpretation.

The simultaneous iterative reconstruction technique, using a modified orthogonal reconstruction method for forming the initial planes, shows good least-error convergence (3–5) requiring approximately seven iterations to achieve 90% reduction in sum of the squared element differences between the original views and the ray-sum views. Approximately 1 hr of computer time was required for image reconstruction. Of note, the iterative process has been observed not only to normalize visually abnormal initial images but also to demonstrate abnormal

sections from views that initially looked normal, as seen in Fig. 6. A slightly revised algorithm using a single iteration and requiring 5 min of computer time is currently used, with comparable results.

The tomographic sections of the stacked-ring phantom show good ring separation consistent with the measured 1.5-cm FWHM depth resolution. The images do show, however, the effect of distance-related size distortion, with the proximal ring appearing as large as the distal one despite 30% actual size variation.

Our criterion for abnormal nontomographic scintigrams—30% minimum-to-maximum count-density variation—is somewhat higher than that found by Sawayama et al. (6), namely, 23% for maximum-to-minimum myocardial count-density separation between normal and abnormal resting Tl-201 scintigrams. Buell et al. (7) used 23–25% for exercise

studies. In our present series, however, the areas of interest considered are smaller than in the others. Due to the tomographic effect and background subtraction, up to 55% minimum-to-maximum count-density variation was found in exercised normal individuals by tomography, frequently due to visualization of detail (such as the aortic valve) not usually seen with standard scintigraphy. This significant degree of normal variation requires visual interpretation of tomographic scintigrams to be done with great caution. The small number (6%) of abnormal Tl-201 stress parallel-hole scintigrams in normal individuals agrees with the results of Bailey et al. (8) and Ritchie et al. (9), who found values of 0% and 4%, respectively. The 72% abnormal nontomographic scintigrams for patients with coronary-artery disease is also quite similar to the 75% and 76% found respectively by these authors. The 92% abnormal tomographic scintigrams among the patients with coronary-artery disease demonstrates increased technique sensitivity, consistent with the findings of Cantez et al. (10). The 10-min delay in obtaining the standard images compared with the tomographic image allows approximately 5% redistribution of Tl-201, which makes this a relatively unimportant factor (11). Chi-squared analysis shows the tomographic data to agree significantly better with the results of angiography (P < 0.05).

In summary, a new method of planar emission tomography, using a standard wide-field Anger scintillation camera and a seven-pinhole collimator, is presented. It demonstrates good phantom imaging characteristics and improved accuracy in clinical diagnostic cardiac perfusion compared with nontomographic scintigraphy.

FOOTNOTE

* Digital Equipment Corporation PDP-12, Maynard, Mass.

REFERENCES

1. KUHL DE, EDWARDS RQ: Image separation radioisotope scanning. Radiology 80: 653–662, 1963

2. MUEHLLEHNER G: Rotating collimator tomography. J Nucl Med 11: 347, 1970 (Abst)

3. GILBERT P: Iterative methods for the three-dimensional reconstruction of an object from projections. J Theor Biol 36: 105–117, 1972

4. LAKSHMINARAYANAN AV, LENT A: The simultaneous iterative reconstruction technique as a least-squares method. SPIE Optical Instrumentation in Medicine V 96: 108–116, 1976

5. BROOKS RA, DI CHIRO G: Principles of computer assisted tomography (CAT) in radiographic and radioisotopic imaging. Phys Med Biol 21: 689–732, 1976

6. SAWAYAMA T, ITO Y, ICHIKAWA T, et al: Thallium-201 imaging with color display computer system in old myocardial infarction. Am J Cardiol 40: 277–281, 1977

7. BUELL U, STRAUER BE, WITTE J: Segmental analysis of Tl-201 stress myocardial scintigraphy: the problem of using uniform normal values of Tl-201 myocardial uptake. J Nucl Med 18: 1240–1241, 1977

8. BAILEY IK, GRIFFITH LSC, ROULEAU J, et al: Thallium-201 myocardial perfusion imaging at rest and during exercise. Comparative sensitivity to electrocardiography in coronary artery disease. Circulation 55: 79–87, 1977

9. RITCHIE JL, TROBAUGH GB, HAMILTON GW, et al: Myocardial imaging with thallium-201 at rest and during exercise: comparison with coronary arteriography and resting and stress electrocardiography. Circulation 56: 66–71, 1977

10. CANTEZ S, HARPER PV, ATKINS F, et al: Tomography in cardiac imaging. J Nucl Med 18: 642, 1977 (Abst)

11. POHOST GM, ZIR LM, MOORE RH, et al: Differentiation of transient ischemic from infarcted myocardium by serial imaging after a single dose of thallium-201. Circulation 55: 294–302, 1977